Live rubella virus vaccine long-term persistence as an antigenic trigger of cutaneous granulomas in patients with primary immunodeficiency

C. Bodemer[1,2,3], V. Sauvage[4], N. Mahlaoui[5,6], J. Cheval[4], T. Couderc[8,9], S.Leclerc-Mercier[1,2,10], M. Debré[5], I. Pellier[11], L. Gagnieur[12], S. Fraitag[2,10], A. Fischer[3,5,6,7], S. Blanche[3,5,6], M. Lecuit[3,6,8,9,13] and M. Eloit[4,12,14]

1) *Department of Dermatology, Necker-Enfants Malades University Hospital, APHP,* 2) *Reference Centre for Cutaneous Rare Diseases (MAGEC),* 3) *Sorbonne Paris Cité, Université Paris Descartes, Institut Imagine,* 4) *PathoQuest, Bâtiment François Jacob,* 5) *Paediatric Haemato-Immunology Unit, Necker-Enfants Malades University Hospital, APHP,* 6) *National Reference Centre for Primary Immune Deficiencies (CEREDIH), Necker-Enfants Malades University Hospital, APHP,* 7) *Inserm U768,* 8) *Institut Pasteur, Biology of Infection Unit,* 9) *Inserm U1117,* 10) *Pathology Department, Necker-Enfants Malades University Hospital, APHP,* 11) *Haematology*–Immunology–Oncology Paediatric Unit, Centre Hospitalier Universitaire d'Angers, Angers, 12) *Institut Pasteur, Department of Virology, Laboratory of Pathogen Discovery,* 13) *Division of Infectious Diseases and Tropical Medicine, Necker-Enfants Malades University Hospital, APHP, Paris and* 14) *Ecole Nationale Vétérinaire d'Alfort UMR 1161 Virologie ENVA, INRA, ANSES, Maisons Alfort, France*

Abstract

Granulomas may develop as a response to a local antigenic trigger, leading to the activation of macrophages and T-lymphocytes. Primary immunodeficiency (PID) is associated with the development of extensive cutaneous granulomas, whose aetiology remains unknown. We performed high-throughput sequencing of the transcriptome of cutaneous granuloma lesions on two consecutive index cases, and RT-PCR in a third consecutive patient. The RA27/3 vaccine strain of rubella virus—the core component of a universally used paediatric vaccine—was present in the cutaneous granuloma of these three consecutive PID patients. Controls included the healthy skin of two patients, non-granulomatous cutaneous lesions of patients with immunodeficiency, and skin biopsy samples of healthy individuals, and were negative. Expression of viral antigens was confirmed by immunofluorescence. Persistence of the rubella vaccine virus was also demonstrated in granuloma lesions sampled 4–5 years earlier. The persistence of the rubella virus vaccine strain in all three consecutive cutaneous granuloma patients with PID strongly suggests a causal relationship between rubella virus and granuloma in this setting.

Original Submission: 5 December 2013; **Revised Submission:** 22 January 2014; **Accepted:** 27 January 2014
Editor: P. Raoult
Article published online: 30 January 2014
Clin Microbiol Infect 2014; **20**: O656–O663
10.1111/1469-0691.12573

Corresponding author: M. Eloit, Institut Pasteur, Laboratory of Pathogen Discovery, Department of Virology, 28 rue du Docteur Roux, F-75724 Paris, France
E-mail: marc.eloit@pasteur.fr

Introduction

Primary immunodeficiency (PID) leads to increased susceptibility to infections. Granuloma is a histopathological term that defines a polymorphic inflammatory infiltrate with a predominance of macrophages. According to its organization and the presence of necrosis, various types of granuloma have been described, which are associated with infections such as mycobacteriosis, and inflammatory diseases such as sarcoidosis [1]. Granulomas may develop in adults with primary immunodeficiency, such as common variable immunodeficiency. In contrast, <50 cases of cutaneous granuloma in paediatric PID patients have been reported so far, only as short series [2,3] or case reports [4] in patients with T-cell immunodeficiencies such as Rag deficiencies, cartilage hair hypoplasia [3], and ataxia telangiectasia (AT) [5]. AT is a recessive autosomal condition caused by loss of function mutations of the *ATM* gene, which encodes a protein kinase that plays a major role in the repair of dsDNA breaks. AT is characterized by developmental abnormalities, neurodegenerative disease, combined immunodeficiency, and a predisposition to malignancies. In the context of AT, skin granuloma is evocative of an underlying opportunistic infection, but

prolonged, broad-spectrum antimicrobial therapy has never led, in our experience and to our knowledge, to any improvement. Moreover, repeated microbial cultures and targeted PCR for uncultivable bacteria or viruses of skin samples have always given negative results ([2] and our unpublished results).

In order to identify putative infectious agents associated with cutaneous granuloma in the context of PID, we subjected cutaneous skin biopsy samples to high-throughput sequencing (HTS). This method consists of sequencing all of the RNAs of a biological sample and sorting these millions of short reads to identify sequences of DNA and RNA viruses, bacteria, fungi, and parasites. Its fundamental advantage is high sensitivity without any *a priori* targets [6].

To our surprise, in three children with PID and cutaneous granuloma who we investigated, we consecutively detected sequences corresponding to a strain similar to the rubella virus (RV) vaccine Wistar RA 27/3 strain and different from the current circulating genotypes. Its presence was confirmed by RT-PCR and immunohistology. Healthy skin of two available index patients with granulomas and control skin samples of immunodeficient patients without granuloma and immunocompetent individuals with or without granuloma were all negative. These results indicate that the RV RA 27/3 vaccine strain persists in the skin of patients with PID, and that this persistence may favour the development of granuloma in the context of PID.

Materials and Methods

Case reports

Patient 1 was a 9-year-old girl with AT. Cutaneous nodules occurred on the buttocks at around the age of 18 months, and later spread to the limbs, trunk, and face. A skin biopsy performed at the age of 3 years confirmed the diagnosis of granuloma, with sarcoidosic, indifferent and lepromatous features according to Ackerman's classification [1]. The inflammatory infiltrate was polymorphic with a predominance of histiocytes and a minor population of lymphocytes, mostly $CD8^+$. No infectious agent was identified by culture or PCR. A clinical and genetic diagnosis of AT was made at the age of 4 years, because of AT clinical features and immunodeficiency with undetectable plasma levels of IgG and IgA (<0.36 g/L and <0.06 g/L, respectively), normal plasma levels of IgM (0.42 g/L), and mild lymphopenia (1290 lymphocytes/mm^3) with a low count of naive $CD4^+$ T-lymphocytes. Immunoglobulin replacement therapy was started, in association with sulphamethoxazole–trimethoprim and azithromycin prophylaxis. The patient received iterative antibiotic treatments for severe interstitial chronic pneumonia, and her clinical status deteriorated progressively. A new skin biopsy was performed at the age of 9 years, with the same findings of intricate granuloma types (Fig. 1a–c), and the sample was subjected to HTS. In the following months, the patient was diagnosed with diffuse large B-cell lymphoma.

Patient 2 was a 15-year-old boy with molecularly confirmed Simpson–Golabi–Behmel syndrome, an X-linked condition that is caused in some patients, including this one, by mutations in the glypican 3 gene, which is involved in the regulation of cell proliferation [7]. The phenotype is variable, and is characterized by developmental abnormalities. In this patient, these were associated with a complex immune disorder consisting of combined immunodeficiency, lymphoproliferation (pulmonary lymphoid infiltration), and autoimmunity (anaemia). At 14 months of age, he developed recurrent pneumonia and severe virus-associated conditions (chickenpox, herpes simplex, and molluscum contagiosum) in a context of protracted lymphoproliferation. At the age of 11 years, he developed eruptive granuloma, involving the buttocks and limbs, and then the face and trunk. Investigations showed 3800 circulating lymphocytes/mm^3, with 1600 T-lymphocytes (1000 $CD4^+$ and 600 $CD8^+$), polyclonal hypergammaglobulinaemia (IgG level of 16.8 g/L, a normal IgA level (1.52 g/L), and elevated IgM plasma levels (3.2 g/L)) with selective IgG_2 deficiency and altered anti-polysaccharide antibody responses. Treatment consisted of immunoglobulin replacement therapy, and antimicrobial prophylaxis with penicillin, sulphamethoxazole–thrimethoprim, and sirolimus. A skin biopsy confirmed the diagnosis of granuloma (indifferent and non-sarcoidosis type). The cellular population was polymorphic, consisting essentially of histiocytes, with a minor lymphocyte population, mostly $CD8^+$. No infectious agent was identified by culture or PCR. At the age of 14 years, a new skin biopsy sample showing a similar granuloma (Fig. 1d–f) was subjected to HTS, and a 2-mm-diameter biopsy was performed in healthy skin.

Patient 3 was a 5-year-old girl with AT. She developed severe recurrent pneumonia from the age of 6 months, severe chickenpox at 2 years of age, hepatosplenomegaly, and, progressively, ocular telangiectasia and cerebellar ataxia. Treatment consisted of immunoglobulin replacement, and sulphamethoxazole–trimethoprim antimicrobial prophylaxis. Cutaneous granulomas occurred on the knees and elbows at the age of 33 months, spreading progressively to the limbs and buttocks. They consisted of annular, erythemato-squamous papular lesions with atrophic centres and well-limited infiltrated borders. Skin biopsies were performed at the age of 5 years, and confirmed the diagnosis of granuloma, with a polymorphic infiltrate (histiocytes and lymphocytes, mostly

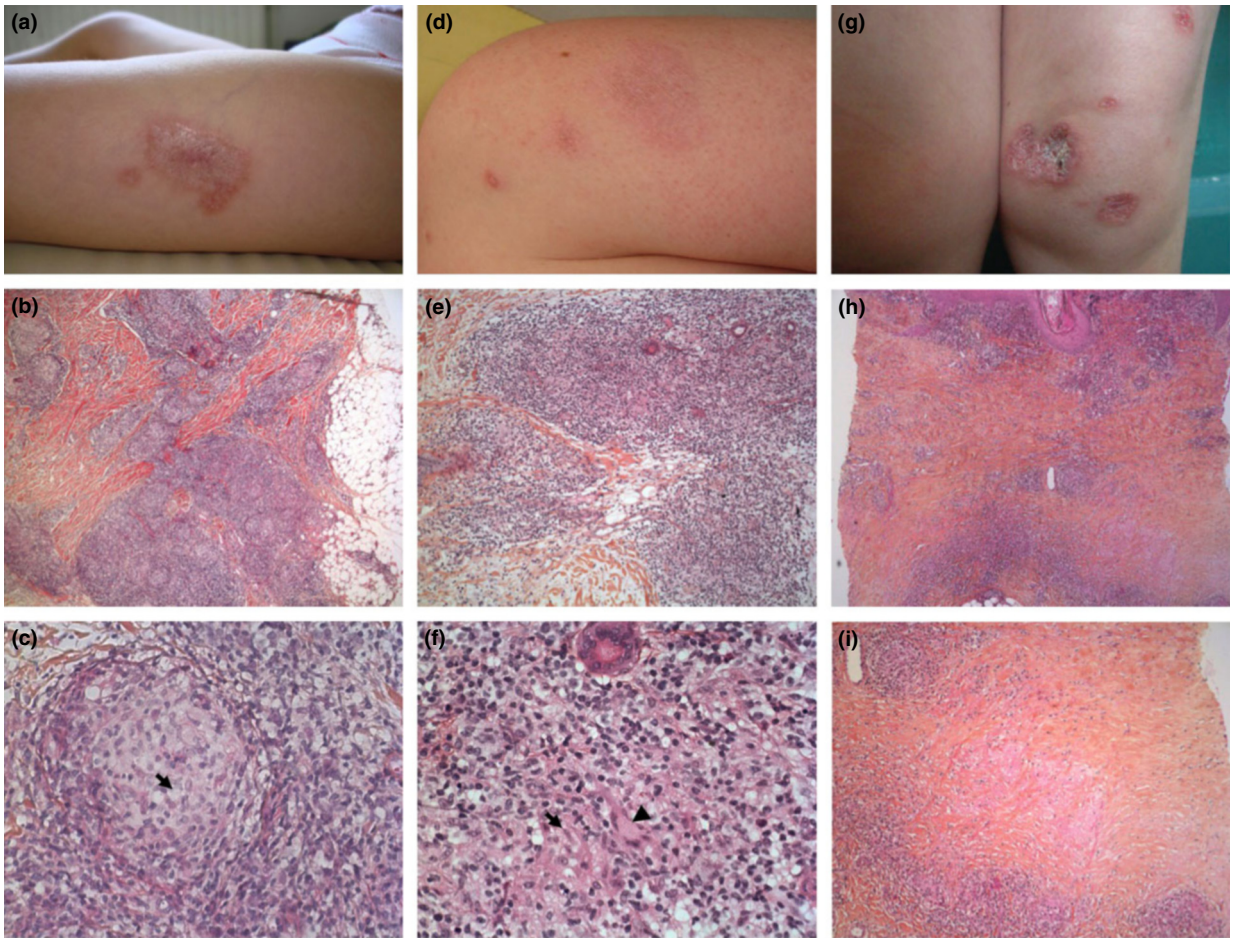

FIG. 1. Clinical cases. Patient 1. (a) Macroscopic aspect of granuloma. (b) Cutaneous granuloma biopsy tissue section, haematein eosin; ×50 magnification. Granulomatous infiltration in an undefined pattern affecting the deep dermis and subcutis. Small, well-limited non-necrotic granulomas are present. (c) Detail of a sarcoidosic granuloma: nodule composed of epithelioid histiocytes (arrow), with lymphocytes around it; ×400 magnification. Patient 2. (d) Infiltrated erythematous plaques. (e) Cutaneous granuloma biopsy tissue section, haematein eosin; ×100 magnification. Granulomatous infiltration of the dermis in an undefined pattern, particularly located around pilo-sebaceous adnexae, composed of lymphocytes and histiocytes. They are arranged in poorly limited tuberculoid granulomas. (f) Infiltration in sweat glands, with some histiocytes. Some of them are epithelioid (arrow), and associated with giant cells (arrowhead); ×400 magnification. Patient 3. (g) Annular lesion with a well-limited infiltrated border and a hyperkeratotic atrophic centre. (h) Skin biopsy: haematein eosin; ×50 magnification. Coexistence of undefined granulomas in the upper dermis and sarcoidal granuloma in the middle dermis. (i) Skin biopsy: haematein eosin; ×100 was the best magnification for observing the coexistence of sarcoidal granuloma in the middle dermis and palisading granulomas in the deep dermis.

$CD8^+$). The coexistence of different types of granuloma was remarkable: undefined granuloma in the upper dermis, sarcoidal granuloma in the middle dermis, and palisading granuloma in the deep dermis. A 2-mm-diameter biopsy was performed in healthy skin. The characteristics of the immunodeficiency were as follows: an IgG level of 1.49 g/L, an IgA level of 1.12 g/L, and a very high IgM plasma level (14.1 g/L); and 980 lymphocytes/mm^3, with low counts of $CD4^+$, naive $CD4^+$, $CD8^+$ and naive $CD8^+$ T-lymphocytes and an absence of proliferation after stimulation with candidin and tetanus toxin. The α-fetoprotein level was elevated, at 55.6 μg/L.

Study design

Skin biopsy samples of patient 1 (sample code 110292) and patient 2 (120479) (index cases) were subjected to HTS analysis independently. On the basis of the initial results, another case (patient 3) was included, and additional samples from these patients were analysed with RT-PCR for specific target amplification, including lymphomatous lymph node biopsy samples, earlier skin biopsy samples, and biopsy samples from healthy skin that could be obtained from patients 2 and 3 (Table 1). As controls, skin biopsy samples from five additional patients were also studied: (i) three from patients with

TABLE 1. Samples, clinical settings, and RT-PCR results

Patient condition	Birthdate, rubella vaccination	Sex	Sampling date	Ru4f/Ru3r PCR	8669F/SPR8 PCR
Granulomatous lesions of the skin associated with immunodeficiency					
Patient 1 (915 U 18 001): ataxia telangiectasia	13 October 2002, Priorix (20 February 2004)	F			
Granuloma biopsy (110292)*			11 May 2011	Positive	Positive
Granuloma biopsy (P9)			3 May 2006	Negative	Positive
Lymph node biopsy (P8)			28 September 2011	Negative	Positive
Plasma			11 May 2011	Negative	Negative
Serum			11 May 2011	Negative	Negative
Patient 2 (915 U 18 002): Simpson–Golabi–Behmel syndrome	21 February 1997, ROR VAX (13 March 1998), Priorix (21 September 2002	M			
Granuloma biopsy (120479)*			15 February 2012	Positive	Positive
Healthy skin biopsy (P6)			15 May 2013	Negative	Negative
Granuloma biopsy (P5)			23 January 2008	Negative	Positive
Plasma			15 February 2012	Negative	Negative
Patient 3 (915 U 18 011): ataxia telangiectasia	15 June 2008	F			
Granuloma biopsy (S-13-0089)	MMRvaxProR (18 November 2009)		22 May 2013	Negative	Positive
Healthy skin biopsy (S-13-0088)	MMRvaxProR (11 October 2010)		22 May 2013	Negative	Negative
Non-granulomatous lesions of the skin with immunodeficiency					
Patient 4 (915 U 18 007): dyskeratosis congenita	8 March 1994, ROR (9 May 1995	M			
Skin biopsy			11 March 2010	Negative	Negative
Patient 5 (915 U 18 008): unclassified combined immunodeficiency	30 June 1969, ROR (1970)	F			
Skin biopsy			1 April 2004	Negative	Negative
Patient 6 (915 U 09 001): acquired immunodeficiency	24 January 1946, unknown				
Skin biopsy (P3)			9 April 2013	Negative	Negative
Healthy immunocompetent patient with normal skin					
Patient 7 (915 U 18 005)	30 December 2008, Priorix (30 September 2010; 8 October 2011	M			
Skin biopsy			27 September 2012	Negative	Negative
Patient 8 (915 U 18 006)	18 July 2008	F			
Skin biopsy	Priorix (3 August 2009; 8 October 2010)		27 September 2012	Negative	Negative

F, female; M, male. *Index cases subjected to high-throughput sequencing analyses.

immunodeficiency showing non-granulomatous skin lesions, in the context of dyskeratosis congenita with severe active chronic skin graft-versus-host disease (patient 4), unclassified combined immunodeficiency with severe eczematous erythroderma (patient 5), and acquired immunodeficiency with verruquous cutaneous lesion of chronic chickenpox (patient 6); and (ii) two from patients without immunodeficiency, managed for nevus resection with excision limits in healthy skin and normal skin controls (patients 7 and 8). All patients had been vaccinated with a live rubella vaccine during their first year of life (Table 1). All patients or parents of children gave written informed consent for the use of these samples, which were used in conformity with French legislation.

HTS and bioinformatics analysis

Total RNA was extracted from biopsy samples or slide sections in TRIzol (Life Technologies, Saint Aubin, France), using for biopsies only a FastPrep system (MP Biomedicals, Santa Ana, CA, USA), and purified with a QiagenMinelute spin column treated with DNase I (Qiagen, Valencia, CA, USA) to digest genomic DNA, as recommended. cDNA synthesis was performed with random hexamers and Superscript III reverse transcriptase (Invitrogen, Saint Aubin, France). Ligation of cDNA, nucleic acid amplification by the bacteriophage Phi29 polymerase, sequencing and bioinformatics analysis were performed as previously described [8]. Reads were generated on an Illumina HiSeq-2000 sequencer (GATC Biotech AG, Konstanz, Germany) with a sequencing depth of 80×10^6 and 148×10^6 paired-end reads of 101 nucleotides for patients 1 and 2, respectively.Sequences were trimmed and filtered according to their quality score. After human genome sequence subtraction (from NCBI build 37.1/assembly hg19) with SOAPaligner and BlastN, reads were assembled in contigs by CLC Genomics (Cambridge, MA, USA), and contigs and singletons were assigned a given taxonomy by use of the nucleotidic and proteic Blast algorithm, with e-values of, respectively, 10^{-3} and 10.

RV detection by RT-PCR and strain typing

Total RNA was reverse transcribed with random primers (patients 1 and 2) or primer Ru1R [9] (patient 3) and Superscript III reverse transcriptase, and digested with RNase H according to the manufacturer's instructions (Invitrogen). For RV E1 gene amplification, two primers, Ru4f and Ru3r [9], were used to generate an 860-nucleotide fragment (nucleotides 8687–9546; GenBank accession number L78917) covering the 739-nucleotide minimum window recommended by the WHO for genotyping (nucleotides 8731–9469) [10]. A second pair of primers, 8669F and SPR8 [11] (nucleotides 8669–9112), that only partially covered the739 nucleotides was used when the previous primer pair failed to amplify.

RV detection by immunofluorescence

Cryosections were labelled with a goat polyclonal antibody against RV (20-RG04; Fitzgerald, Wicklow, Ireland), and then with a secondary antibody coupled to Alexa-546. Slides were counterstained with Hoechst (Vector Laboratories, Burlingame, CA, USA) and observed under an AxioObserver microscope (Zeiss, Oberokochen, Germany). Pictures and Z-stacks were obtained with AxioVision 4.5 software.

Results

A cutaneous granuloma biopsy sample (110292) from patient 1 was subjected to HTS, with the aim of identifying a potential associated pathogen. Among a total of 80 million reads, four contigs (149–240 bp; Fig. 2a) and 43 singletons (31–101 bp; not shown) gave as best hits sequences of a known virus, the Wistar 27/3 attenuated RV strain (FJ211588), which most countries use as a live attenuated vaccine, and the five rubella vaccine strains used in Japan (Matsuba.GMK3 (AB588189), TCRB19 (AB588188), Matsuura (AB588191), TO-336.GMK5 (AB588192), and Takahashi (AB222608)). These contigs and singletons showed a minimum of 98% and 96% nucleotide identity, respectively, with the cited rubella vaccine strains. No other viral read was found.

We next investigated patient 2. A skin biopsy sample (120479) was sequenced with a greater depth (148 million reads), and 21 contigs (102–584 bp; Fig. 2a) and 34 singletons (32–101 bp; not shown) matched the rubella vaccine strains mentioned above, with nucleotide identities ranging from 97% to 100%. RV contigs covered approximately 46% of the 9762-bp reference genome of the Wistar 27/3 strain (FJ211588) (Fig. 2a). Within the E1 window for rubella genotyping recommended by the WHO, two contigs of 232 bp and 122 bp showed 99% and 100% identity with the Wistar 27/3 vaccine strain. No other viral read was found.

RT-PCRs were performed with specific primers amplifying more than the minimal 739 nucleotides of the E1 envelope coding region, which is used for strain typing according to WHO recommendations. For the biopsy samples of two patients (110292 and 120479), the results were positive (Table 1; Fig. 2b), and Sanger sequencing confirmed the presence of a genotype 1a virus that circulates neither in France nor in most other countries, with a sequence very close to that of the Wistar 27/3 vaccine strain FJ211588 (Tables S1 and S2; Figs S1, S2, and S4). RT-PCR was negative for a biopsy sample of healthy skin of patient 2; the corresponding control in patient 1 was not available.

Immunofluorescence with an anti-RV polyclonal antibody revealed the presence of RV antigens in cells of deep dermis granuloma (Fig. 2) that were vimentin-positive (not shown). The strain was also detected by RT-PCR for both patients in granuloma biopsy samples obtained 4–5 years before and in the lymphomatous lymph node biopsy sample of patient 1 obtained 4 months later (Table 1; Figs S3 and S5). Anti-RV immunofluorescence was negative on the RT-PCR-positive lymphomatous lymph node (not shown). Concomitant plasma and serum samples were negative (Table 1).

We next investigated the granuloma biopsy sample (S-13-0089) of the third child with PID and granuloma, referred to us in the course of this study. RT-PCR was positive for the granuloma sample and negative for the healthy skin. Sanger sequencing revealed the presence of a genotype 1a virus with a sequence very close to that of the Wistar 27/3 vaccine strain FJ211588 (Table S3; Fig. S6).

As control, skin biopsy samples from three immunosuppressed and rubella-vaccinated patients with inflammatory non-granuloma lesions (graft-versus-host disease, eczematous lesions, and chronic chickenpox; patients 4, 5, and 6), and two immunocompetent healthy children (patients 7 and 8) were analysed for the presence of RV RNA. All were negative (Table 1; Fig. 2b).

Discussion

We report here three cases of cutaneous granuloma associated with rubella vaccine related-strains in patients with PID. It is of note that these three cases were referred to our centre consecutively, that their initial extensive microbiology work-up gave completely negative results, but that all of them turned out to be positive for RV, suggesting a very strong association between RV and skin granuloma in children with PID. Granulomatous lesions are composed of inflammatory cells, including macrophages. Granuloma may develop as a response to a local trigger, leading to the activation of macrophages that can show features of epithelioid and giant cells, and T-lymphocytes. Granulomas develop as a result of infectious or non-infectious antigenic triggers, whose persistence favours granuloma development. This accounts for the facts that: (i) pathogens associated with granulomas usually cause chronic infection and persist within the host; and (ii) conditions associated with continuous antigenic triggering and a lack of antigen clearance lead to granuloma formation. T-cell responses are important in granuloma formation, and patients with deficient T-cell functions are less likely to develop granulomas [12], except those with eruptive granuloma annulare (GA) [13]. GA also occurs in immunocompetent patients, in whom it shows a palisade aspect and is usually non-eruptive. Members of the family *Herpesviridae*

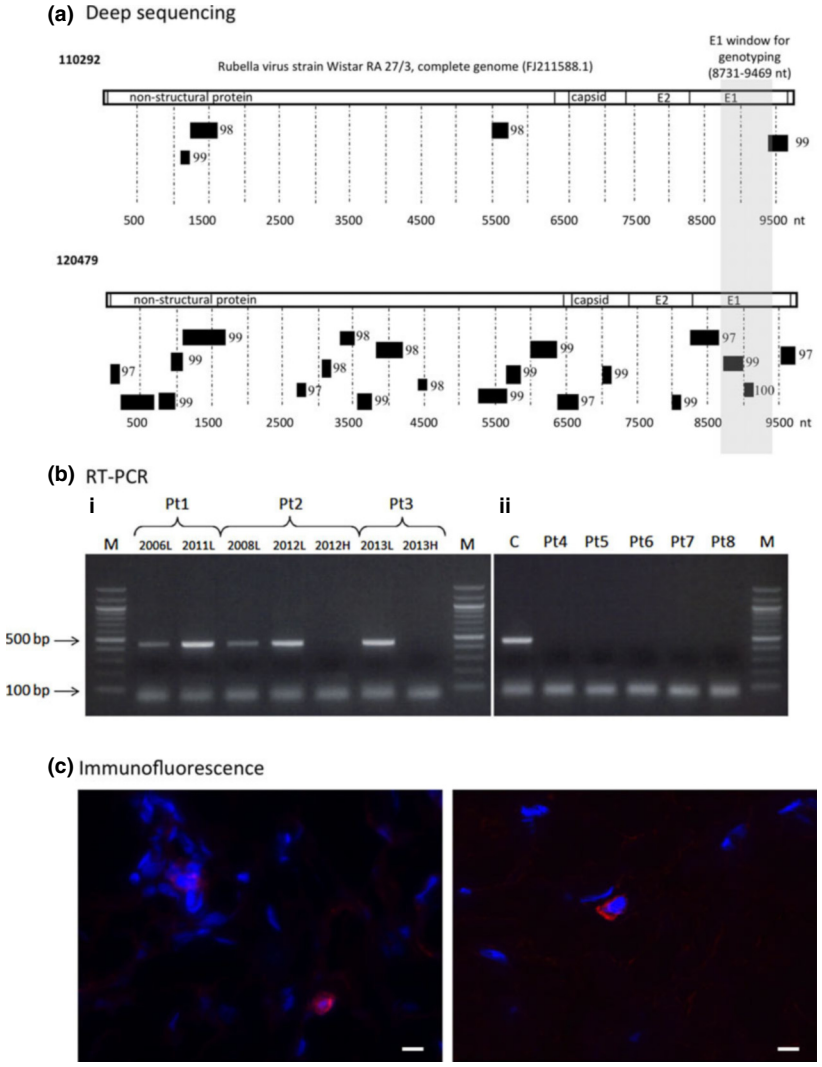

FIG. 2. High-throughput sequencing, RT-PCR and immunofluorescence of cutaneous granuloma biopsy samples. (a) Contigs identified by deep sequencing in granuloma biopsy samples of patient 1 (110292) and patient 2 (120479) are shown, together with a genomic map of the strain Wistar RA 27/3 (FJ211588). Each contig is represented by a horizontal bar together with the percentage of identity with the reference genome. For clarity, singletons are not shown. (b) Results of RT-PCR with the primers 8669F and SPR8 are shown for (i) lesion (L) or healthy skin (H) biopsy samples of the three index cases (patient (P)t1 to Pt3, with the corresponding year of sampling) and (ii) the five controls (Pt4 to Pt8). C: positive control. M: 100-bp ladder. (c) Tissue sections of cutaneous granuloma frozen biopsy samples of patient 1 (left panel) and patient 2 (right panel) immunolabelled with an anti-rubella polyclonal antibody and double-labelled with a secondary antibody coupled to Alexa-546. RV-positive cells appear in red; nuclei are stained with Hoechst, and appear in blue. Fewer than one positive cell per field and no cluster of positive cells were observed. Control RV RT-PCR negative tissues were all RV-negative by immunofluorescence. Bar: 10 μm.

have been proposed as triggers in patients with eruptive GA [14–16].

RV can be isolated from the skin during the acute phase of rubella, even in the absence of rash [17]. RV persists in the skin in congenital rubella, and this is attributed to a relatively high tolerance to viral proteins expressed during fetal life [18].

We show here that RV has persisted for several years in disseminated granulomas of unknown aetiology in all three young patients with PID. The three virus strains are of genotype 1a, and, although they are different from currently circulating strains [11], they are closely related to the Wistar 27/3 strain used in the vaccines from the two known manufacturers, from which they were most likely derived, subsequent to vaccination years before. The presence of RV antigens was shown by immunofluorescence (Fig. 2c), and therefore they may well represent a persistent antigenic

trigger that promoted granuloma formation. Although we cannot definitely exclude a bystander effect for this skin-tropic virus, its absence in healthy skin samples distant from granuloma lesions and the serum of index cases rules out widespread dissemination of RV in a context of immunodeficiency, and strongly supports a causal role for RV in granuloma formation in paediatric PID. In support of this hypothesis, RV was absent in control patients 4 and 5 with immunodeficiency and non-granulomatous inflammatory skin lesions, suggesting that RV is not detectable in all skin samples of immunosuppressed patients, and is not a triggering factor for such lesions.

It is of note that RV was also present in a lymphomatous adenopathy in patient 1 but RV-expressing cells were not identifiable by immunofluorescence. Further investigations are therefore needed to investigate a possible link between RV and the development of lymphoma in this patient with AT, a condition associated with a high risk of neoplasia, mainly lymphoma. RV replicates in monocytes and also in activated B-lymphocytes and T-lymphocytes [19,20]. Long-term viraemia occurs in the context of congenital infection [21], and live vaccine strains replicate in lymphocytes of immunocompetent vaccinized individuals for several weeks [22]. RV capsid inhibits Fas-dependent apoptosis mediated by Bax, and it has been suggested that this may allow within-host viral dissemination by way of apoptosis-resistant infected lymphocytes [23]. ATM is one of the major kinases of the DNA damage response, and Bax is also a component of the ATM signalling machinery in some cell types [24], implying that ATM loss of function and RV-associated Bax impairment could act synergistically to avoid apoptosis, thereby favouring lymphoma development. In addition, RV proteins may also act as a persistent antigenic trigger that favours protracted lymphocyte activation and accumulation of DNA damage. Lymphomas in AT patients were described before the widespread use of rubella vaccines, but the incidence of rubella was very high before vaccine implementation, permitting a significant exposure of AT patient to RV [25].

Detection of the vaccine strain of RV in all three consecutive cases strongly suggests a causal relationship between RV and granuloma in patients with PID. Indeed, most of Hill's criteria [26] for causation are fulfilled: association, specificity, temporality (all these three patients were vaccinated before the appearance of the granulomas, and RV persisted for years in the lesions), and plausibility. A demonstration of causality will nevertheless require multicentric prospective series of cases.

Our findings suggest that granulomas and lymphomas occurring in the context of immunodeficiency should be investigated for the presence of RV. The general population is widely exposed to live rubella vaccine, including immunocompromised patients, and more particularly those with PID, who are frequently unknowingly immunosuppressed at the time of vaccination. It should be noted, however, that, in the absence of widespread vaccination, patients with PID would probably be exposed to non-attenuated RV, owing to circulating wild-type RV.

This study has identified RV as a likely cause of cutaneous granuloma in children with PID. It illustrates the strength of deep sequencing in revealing the presence of unpredicted infectious agents in patients' tissue samples, and in uncovering their putative role in poorly understood medical conditions. The increasing use of HTS in clinics should be applied to pathological tissue samples of patients with unknown medical conditions, to search for associated infectious agents.

Acknowledgements

This work received financial support from Institut Pasteur, Labex IBEID, Inserm, Fondation BNP-Paribas, Ville de Paris, the European Research Council, and a specific grant from ANR, project INF-ID-KIDS (France). We thank N. Corre-Catelin (Icareb, Institut Pasteur, Paris) for her help with the management of the biological samples.

Transparency Declaration

V. Sauvage and J. Cheval are employees and M. Eloit is the chairman of pathoquest.

Supporting Information

Additional Supporting Information may be found in the online version of this article:

Data S1. Rubella virus sequences analysis

References

1. Ackerman B. Histologic diagnosis of inflammatory skin diseases. *Histologic diagnosis of inflammatory skin diseases*, 3rd edn. NY: Ardor Scribendi, 2005; pp.552.
2. Paller AS, Massey RB, Curtis MA *et al.* Cutaneous granulomatous lesions in patients with ataxia-telangiectasia. *J Pediatr* 1991; 119: 917–922.
3. Moshous D, Meyts I, Fraitag S *et al.* Granulomatous inflammation in cartilage-hair hypoplasia: risks and benefits of anti-TNF-α mAbs. *J Allergy Clin Immunol* 2011; 128: 847–853.
4. Schuetz C, Huck K, Gudowius S *et al.* An immunodeficiency disease with RAG mutations and granulomas. *N Engl J Med* 2008; 358: 2030–2038.

5. Chiam LYT, Verhagen MMM, Haraldsson A *et al.* Cutaneous granulomas in ataxia telangiectasia and other primary immunodeficiencies: reflection of inappropriate immune regulation? *Dermatology (Basel)* 2011; 223: 13–19.
6. Lipkin WI. The changing face of pathogen discovery and surveillance. *Nat Rev Microbiol* 2013; 11: 133–141.
7. Pilia G, Hughes-Benzie RM, MacKenzie A *et al.* Mutations in GPC3, a glypican gene, cause the Simpson–Golabi–Behmel overgrowth syndrome. *Nat Genet* 1996; 12: 241–247.
8. Cheval J, Sauvage V, Frangeul L *et al.* Evaluation of high-throughput sequencing for identifying known and unknown viruses in biological samples. *J Clin Microbiol* 2011; 49: 3268–3275.
9. Feng Y, Santibanez S, Appleton H, Lu Y, Jin L. Application of new assays for rapid confirmation and genotyping of isolates of rubella virus. *J Med Virol* 2011; 83: 170–177.
10. World Health Organization. Standardization of the nomenclature for genetic characteristics of wild-type rubella viruses. *Wkly Epidemiol Rec* 2005; 80: 126–132.
11. Vauloup-Fellous C, Hübschen JM, Abernathy ES *et al.* Phylogenetic analysis of rubella viruses involved in congenital rubella infections in France between 1995 and 2009. *J Clin Microbiol* 2010; 48: 2530–2535.
12. Aftergut K, Cockerell CJ. Update on the cutaneous manifestations of HIV infection. Clinical and pathologic features. *Dermatol Clin* 1999; 17: 445–471, vii.
13. Toro JR, Chu P, Yen TS, LeBoit PE. Granuloma annulare and human immunodeficiency virus infection. *Arch Dermatol* 1999; 135: 1341–1346.
14. Serfling U, Penneys NS, Zhu WY, Sisto M, Leonardi C. Varicella-zoster virus DNA in granulomatous skin lesions following herpes zoster. A study by the polymerase chain reaction. *J Cutan Pathol* 1993; 20: 28–33.
15. Redondo P, España A, Sola J, Rocha E, Quintanilla E. Sarcoid-like granulomas secondary to herpes simplex virus infection. *Dermatology (Basel)* 1992; 185: 137–139.
16. Nikkels AF, Debrus S, Delvenne P *et al.* Viral glycoproteins in herpesviridae granulomas. *Am J Dermatopathol* 1994; 16: 588–592.
17. Heggie AD. Pathogenesis of the rubella exanthem: distribution of rubella virus in the skin during rubella with and without rash. *J Infect Dis* 1978; 137: 74–77.
18. Mauracher CA, Mitchell LA, Tingle AJ. Selective tolerance to the E1 protein of rubella virus in congenital rubella syndrome. *J Immunol* 1993; 151: 2041–2049.
19. Van der Logt JT, van Loon AM, van der Veen J. Replication of rubella virus in human mononuclear blood cells. *Infect Immun* 1980; 27: 309–314.
20. Chantler JK, Tingle AJ. Replication and expression of rubella virus in human lymphocyte populations. *J Gen Virol* 1980; 50: 317–328.
21. Jack I, Grutzner J. Cellular viraemia in babies infected with rubella virus before birth. *Br Med J* 1969; 1: 289–292.
22. Buimovici-Klein E, Cooper LZ. Immunosuppression and isolation of rubella virus from human lymphocytes after vaccination with two rubella vaccines. *Infect Immun* 1979; 25: 352–356.
23. Ilkow CS, Goping IS, Hobman TC. The rubella virus capsid is an anti-apoptotic protein that attenuates the pore-forming ability of Bax. *PLoS Pathog* 2011; 7: e1001291.
24. Chong MJ, Murray MR, Gosink EC *et al.* Atm and Bax cooperate in ionizing radiation-induced apoptosis in the central nervous system. *Proc Natl Acad Sci USA* 2000; 97: 889–894.
25. Plotkin SA. The history of rubella and rubella vaccination leading to elimination. *Clin Infect Dis* 2006; 43 (suppl 3): S164–S168.
26. Rothman KJ, Greenland S. Causation and causal inference in epidemiology. *Am J Public Health* 2005; 95 (suppl 1): S144–S150.